EurJOC European Journal of Organic Chemistry

SHORT COMMUNICATION

DOI: 10.1002/ejoc.201402845

Infrared Multiphoton Dissociation Spectroscopic Analysis of Noncovalent Interactions in Organocatalysis

Mareike C. Holland,[a,b] Giel Berden,[c] Jos Oomens,[c,d] Anthony J. H. M. Meijer,*[e] Mathias Schäfer,*[f] and Ryan Gilmour*[a]

Keywords: Organocatalysis / Theoretical chemistry / Conformation analysis / Noncovalent interactions / Infrared multiphoton dissociation spectroscopy

Herein we report the first application of infrared multiple-photon dissociation (IRMPD) spectroscopy to study noncovalent interactions in organocatalysis. Phenylalanine-derived iminium ions, central to numerous organocatalytic processes, display dynamic conformational behavior as a consequence of stabilizing noncovalent interactions (e.g., CH–π, π–π). Electronic modulation of the aryl ring causes notable variation in the conformation; this can be detected spectroscopically and correlated with enantioselectivity. Given that these interactions, which orchestrate stereoinduction, encode for specific conformers (I, II, or III), a diagnostic IRMPD spectrum is generated: the C=O stretching frequency of the imidazole carbonyl group serves as a diagnostic marker. The calculated conformers and their respective spectra can be compared with experimental data. Consequently, valuable insight into the ubiquitous noncovalent interactions associated with MacMillan-catalyst-derived α,β-unsaturated iminium ions can be obtained in the absence of solvent or counterion effects. A preliminary structure–catalysis correlation is disclosed, thus demonstrating the potential of this approach for studying reactive intermediates and facilitating catalyst design.

Introduction

Noncovalent interactions are ubiquitous in protein structural biology and play an integral role in governing conformation and function.[1] Often, these interactions are prevalent in regions of molecular space containing electron-rich amino acid side chains. Although highly preorganized biomolecules offer the possibility to study these interactions closely (Figure 1), the bioinspired nature of many small-molecule organocatalysts offers a structurally simplified platform for their investigation.[1b]

[a] Organisch Chemisches Institut and Excellence Cluster EXC 1003, Cells in Motion, Westfälische Wilhelms-Universität Münster,
Corrensstrasse 40, Münster, Germany
E-mail: ryan.gilmour@uni-muenster.de
www.uni-muenster.de/Chemie.oc/gilmour/
[b] Department of Chemistry and Applied Biosciences, ETH Zürich,
Vladimir-Prelog-Weg 1-5/10, 8093 Zürich, Switzerland
[c] Institute for Molecules and Materials, Radboud University Nijmegen, FELIX Facility,
Toernooiveld 7, 6525 ED Nijmegen, Netherlands
[d] van't Hoff Institute for Molecular Sciences, University of Amsterdam,
Science Park 904, 1098 XH Amsterdam, Netherlands
[e] Department of Chemistry, University of Sheffield,
Sheffield S3 7HF, UK
E-mail: a.meijer@sheffield.ac.uk
[f] Department für Chemie, Universität zu Köln,
Greinstrasse 4, 50939 Köln, Germany
E-mail: mathias.schaefer@uni-koeln.de
Supporting information for this article is available on the WWW under http://dx.doi.org/10.1002/ejoc.201402845.

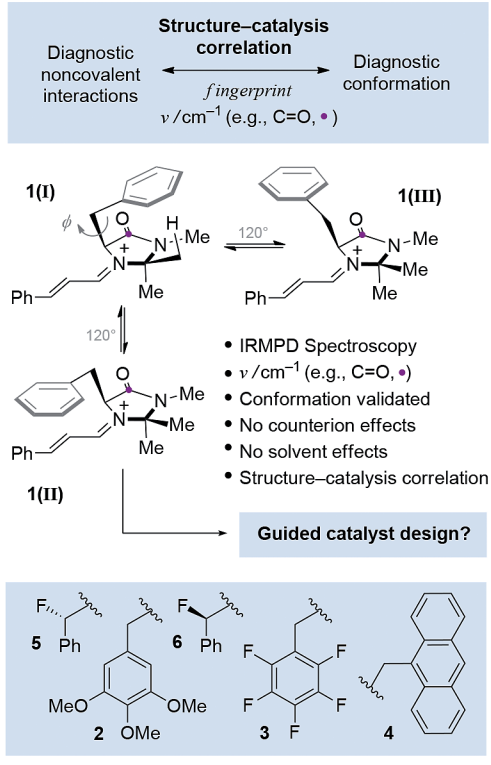

Figure 1. Correlating structure and function in organocatalysis by IR multiple photon dissociation (IRMPD) spectroscopy.

Consequently, the intimate structure–function relationship that is central to structural biology may be effectively

translated into the realm of organocatalysis. The practical value of drawing this parallel manifests itself in a range of catalyst design strategies and reactivity models. This analogy with nature's catalysts is perhaps most obvious upon considering the iminium ion intermediate derived from MacMillan's phenylalanine-derived imidazolidinone catalyst (**1**).[2] The structural rigidity of the catalyst core provides a geometrically optimized platform for the oscillating phenyl ring to engage in a stabilizing CH–π interaction[3] with the *syn* methyl group, a π–π stack with the pendant iminium chain, or even engage in a weak CH–CO van der Waals interaction.[4] Consequently, three staggered conformers partitioned by 60° can be envisaged and correlated with these interactions (Figure 2; **I**, **II**, and **III**). These stabilizing phenomena manifest themselves in the conformations of the reaction intermediates[5] and ultimately play a role in orchestrating selectivity, which further accentuates this structure–function analogy to enzyme catalysis. Understanding the synergy and function of these interrelated conformers remains challenging but will confer practical advantages for future organocatalyst design.

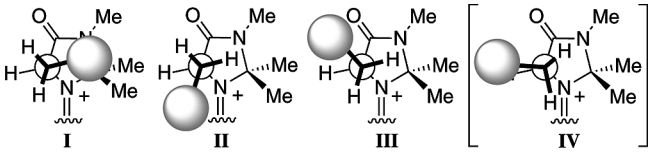

Figure 2. Conformational diversity in MacMillan imidazolidinone-derived iminium ions (**1**): **I** consistent with CH–π interaction, **II** consistent with π–π stack, **III** eclipsed with the carbonyl group, consistent with CH–CO van der Waals interaction, **IV** C–C_{ipso} and C–H bond eclipsed, also with possible CH–CO van der Waals interaction.

Modulating C–C_{ipso} torsional rotation in iminium salts such as **1** can be achieved by inducing electronic perturbations in the aryl shielding group. Indeed, the quadrupole moment (Q_{zz}) of the aryl ring and the enantioselectivity of certain reactions can be correlated.[6] The clear reciprocity between noncovalent interactions in conformers **I** and **II** and effective enantioselective catalysis necessitates the development of structure–function correlation methods. To complement the existing structural analysis methods of computation, NMR spectroscopy and crystallography, IR multiple photon dissociation (IRMPD) spectroscopy was investigated. The gas-phase conditions of this technique would alleviate concerns pertaining to crystal-packing effects influencing conformation and allow the naked iminium ion to be analyzed in the absence of counterions. A major caveat of solution-phase analyses is that counterions are often far from innocent.[7] To realize this goal, a series of iminium salts (i.e., **2**–**6**, Figure 1) was prepared and their IRMPD spectra were recorded.[8] Unlike classical IR spectroscopy, which is not applicable for ions stored in an ion trap, the use of IRMPD spectroscopy[9] has been developed as an effective alternative "action spectroscopy" method.[10] IRMPD spectroscopy combined with theory has proven to be a powerful analytical strategy, especially for cases in which the ions have only a limited number of oscillators that exercise vibrations obeying harmonic approximations.[11] This prerequisite holds true for the MacMillan-type imidazolidinone-derived iminium ions, which are structurally analogous to peptide *b*-type fragment ions; the oxazolone components of these systems have been elucidated by IRMPD spectroscopy.[12] In IRMPD spectroscopy, a given precursor ion is slowly heated by absorption of tens to hundreds of IR photons, for which powerful laser systems are needed.[13] Upon intramolecular vibrational redistribution (IVR), the activated ion finally reaches the critical internal energies of one or more fragmentation pathways and dissociates.[14] Free electron lasers (FEL) are well suited for this experiment and have the capability of continuous wavelength tunability over a wide wavelength range (e.g., 3–250 μm for the FEL used in this study).[15]

In addition to noncovalent hydrogen bonds C=O···HX (X = O, N, C), which lead to a redshift in the C=O stretching mode,[16] weak dispersion forces such as XH···π (X = C, N, O) interactions shift the respective bands and are useful diagnostic features for the identification of individual conformers.[17] It was envisaged that the stretching mode imidazolidinone carbonyl group of **1** would be a sensitive probe from which to investigate changes in conformation resulting from rotation about the C–C(Ph) bond. Importantly, the diagnostic shifts of the C=O stretching modes are expected to be small, as the C=O moieties experience at best only weak interactions, for example, side-on interactions with aromatic substituents or interactions with CH groups. To achieve pronounced electronic changes for this study, iminium salts with vastly differing quadrupole moments were prepared (i.e., **2**, **3**, and **4**; Q_{zz} = –5.68, +3.01, and –7.62, respectively).[18] In addition, conformational equivalents **5** and **6** frozen by virtue of the fluorine-iminium ion *gauche* effect[19] were studied (Figure 1). For all of these compounds, calculation of the lowest-energy conformers (e.g., see Figure 2) were performed by using density functional theory (DFT) with the B3LYP functional[20] and a triple-zeta (6-311G**) basis set[21] as implemented in Gaussian09.[22] These calculations (full details are given in the Supporting Information), together with simulation of their IRMPD spectra would allow for rapid comparison with the experimental data collected from photodissociation experiments generated by the FELIX free-electron laser. Comparison of the observed CO frequencies with calculated values shows a maximum deviation of 6 cm^{-1}. Thus, the conformation of each modified iminium ion could be assigned in the absence of counterions and solvents, which ultimately allows comparison with catalysis findings. Herein, we present a preliminary validation of IRMPD spectroscopy as a powerful method to study noncovalent interactions in organocatalysis and disclose a preliminary structure–catalysis correlation examining the role of these interactions in the Friedel–Crafts alkylation of *N*-methylpyrrole, a transformation that is known to be sensitive to counterion effects.[23,24]

Results and Discussion

As a starting point for this study, electron-rich trimethoxyphenyl derivative **2** was chosen; this derivative is known to significantly populate conformation **I**, which allows for a CH–π interaction with the *syn* Me group. Moreover, conformation **II** is also populated to an extent in solution, which thus directs the aromatic group over the pendant iminium chain. Three energy minima were identified within 3.3 kJ mol^{-1} of the global minimum electronic energy (Figure 3). The global minimum was found to be conformer **II** (Φ_{NCCC} = –78.2°). A structure with the freely rotatable C–C bond to the phenyl group almost eclipsed with the neighboring C–H bond (conformer **IV**, Φ_{NCCC} = –132.2°; see Figure 2) was found to be only 0.08 kJ mol^{-1} higher in energy. This latter conformer was previously reported by Houk and co-workers.[4a] Moreover, Seebach and Grimme reported that these two conformers are connected by an energetic plateau in their "windshield-wiper" model.[25] Insignificantly higher in energy (+0.4 kJ mol^{-1}) is the conformer that is stabilized by a CH–π interaction (i.e., **I**, Φ_{NCCC} = +51.7°). A fourth energy minimum (3.3 kJ mol^{-1} higher in energy) also adopts conformer **II** (Φ_{NCCC} = –71.7°), but with the methoxy groups oriented differently. From this computational analysis it is proposed that the shielding group oscillates freely between Φ_{NCCC} = –132.2° and +51.7°. Comparison of the computed IR spectra for each conformer with the measured IRMPD spectra beautifully illustrates the distributed conformer population of **2**. Whereas the C=O stretching bands corresponding to the two lower lying conformers have very similar frequencies, the measured band is slightly blueshifted owing to non-negligible population of the third conformer in which the weaker H-bond leads to a blueshift in the band. Next, pentafluorophenyl analogue **3** was studied as an electronic extreme of **2**. Previous studies suggest that this iminium ion preferentially adopts conformation **III**,[6] in which the aromatic ring is rotated away from the imidazolidinone core; this brings it in close proximity to the carbonyl group, whereby a CF–CH van der Waals interaction stabilizes this structure. Computational analysis of **3** verified this conformer to be the global minimum structure (Φ_{NCCC} = –168.8°; Figure 3, center left). This is in good agreement with the crystal structure (Φ_{NCCC} = –176.7°).[6]

The second lowest conformer was calculated to be that stabilized by the postulated π–π interaction (i.e., **II**, +7.1 kJ mol^{-1} higher in energy). Higher in energy is the third identified minimum structure (+11.8 kJ mol^{-1}) corresponding to the CH–π conformer (i.e., **I**). Even though the differences in C=O stretching frequencies of the computed IR spectra are subtle, it is clearly visible that the measured IRMPD C=O band fits best to the IR C=O band of the global energy minimum (Figure 3). It is noted that the C_6F_5 breathing motion found at $\tilde{\nu}$ = 1510 cm^{-1} is predicted to be notably redshifted by theory. To probe the effect of steric modification, anthracenyl derivative **4** was also investigated. Examination of the calculated minima structures (Figure 3) revealed that only conformer **II** is significantly populated (Φ_{NCCC} = –77.2°). This is believed to be due to an edge-on interaction between the electron-rich aromatic system and the positively charged iminium chain as well as a CH–CO van der Waals interaction. The other two minima identified, corresponding to the CH–π conformer (i.e., **I**) and the rotamer with the aromatic group in proximity to the carbonyl moiety (i.e., **III**), lie much higher in energy (13.2 and 18.2 kJ mol^{-1}, respectively), which suggests that oscillation of the shielding group is restricted, contrary to the Seebach–Grimme model.[25] This supposition was again verified by IRMPD spectroscopy (Figure 3). The experimentally observed C=O bond stretching frequency matches the calculated value for the global minimum structure, whereas the computed spectra for the other two conformers are both shifted, and this further validates the method. The low experimental intensity of the otherwise strong CH wagging absorption of the aromatic system is presently not well understood.

Finally, iminium ions **5** and **6** were examined by using IRMPD spectroscopy. This laboratory has previously reported that a configurationally defined benzylic fluorine substituent can be exploited to fix the position of the substituents on the fluorine-bearing carbon atom by virtue of the fluorine *gauche* effect [$\sigma_{C-H} \rightarrow \sigma^*_{C-F}$, $F^{\delta-} \cdots N^+$]. Consequently, this steering group can encode for conformer **I** or **II**, depending on the configuration of the stereogenic center. By locking the phenyl group in the π–π conformation (i.e., **6**; **II**) or the CH–π conformation (i.e., **5**; **I**), it is possible to generate diastereomeric "conformer equivalents"[19b] of the two rotamers, which are believed to be important for enantioinduction. As expected, the global minimum of **5** was calculated to be the one allowing for CH–π interaction (i.e., **I**, Φ_{NCCC} = +45.4°; Φ_{NCCF} = –79.0°). Only one other minimum structure was identified (+8.8 kJ mol^{-1} higher in energy), which conceivably would still allow for the same interaction, but with inverted configuration around the C=N$^+$ bond. The gas-phase spectrum matches the computed IR spectrum of the global minimum structure (Figure 3, upper right). For **6**, the calculated lowest-energy conformation (Figure 3, lower right) was found to be the expected *syn*-clinal *endo* conformation (i.e., **II**; Φ_{NCCF} = +48.8°) but distorted in comparison to the X-ray structure, which displayed a perfect *syn*-clinal *endo* conformation (i.e., **II**; Φ_{NCCF} = +64.4°).[19b]

A second low-lying conformer only 1.3 kJ mol^{-1} higher in energy was found to be conformer **IV**, which results in the C–F bond eclipsing the C–N bond of the iminium core (Φ_{NCCC} = –130.7°, Φ_{NCCF} = +7.7°). Once again, comparison of the computed IR spectra for the two conformers with the measured IRMPD spectra confirms these findings, and this beautifully illustrates that the two conformers lie close in energy and that the recorded C=O band lies in the middle of the two calculated for the two isolated conformers. This observation further underscores the need for structural methods to study iminium ions that are complement to crystallographic techniques.[26]

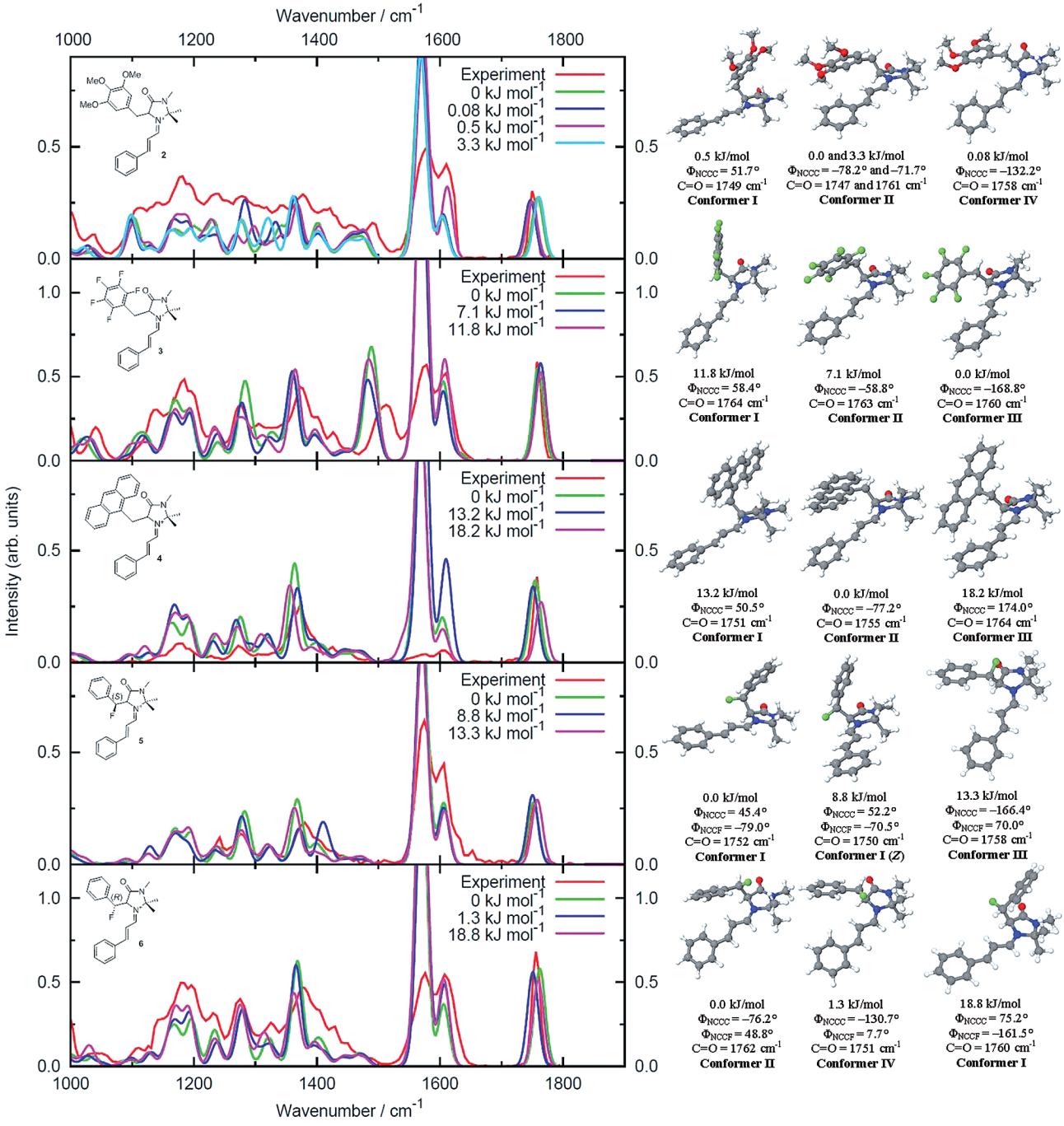

Figure 3. (Left) IRMPD spectrum (red) of **2** overlaid with theoretical spectra of global minimum structure (green) and the other identified energy minima conformations at +0.08 kJ mol^{-1} (blue), +0.5 kJ mol^{-1} (pink) and +3.3 kJ mol^{-1} (turquoise). The three optimized minimum energy conformers and relative energies. IRMPD spectrum (red) of **3** overlaid with theoretical spectra of global minimum structure (green) and the other identified energy minima conformations at +7.1 kJ mol^{-1} (blue) and +11.8 kJ mol^{-1} (pink). The three optimized minimum energy conformers and relative energies. IRMPD spectrum (red) of **4** overlaid with theoretical spectra of global minimum structure (green) and the other identified energy minima conformations at +13.2 kJ mol^{-1} (blue) and +18.2 kJ mol^{-1} (pink). The three optimized minimum energy conformers and relative energies. IRMPD spectrum (red) of **5** overlaid with theoretical spectra of global minimum structure (green) and the other two identified energy minimum conformations at +8.8 kJ mol^{-1} (blue) and +13.3 kJ mol^{-1} (pink). The two optimized minimum energy conformers and relative energies. IRMPD spectrum (red) of **6** overlaid with theoretical spectra of global minimum structure (green) and the other two identified energy minimum conformations at +1.3 kJ mol^{-1} (blue) and +18.8 kJ mol^{-1} (pink). (Right) The optimized minimum energy conformers, torsion angles, calculated frequencies, and relative energies. Calculated frequencies were scaled by 0.97. Each was convoluted with a Gaussian function (full width at half maximum: 15 cm^{-1}) to obtain the theoretical IRMPD spectra.

Finally, in an effort to correlate the IRMPD findings with reaction outcomes, the Friedel–Crafts alkylation of *N*-methylpyrrole was selected as a model transformation. This reaction has previously been reported to be highly suscepti-

ble to counterion effects, solvent effects, catalyst conformation, and electronic nature of the shielding group on the MacMillan catalyst,[6,19b,23,24] which renders it ideal for this analysis. Moreover, a recent study by Sigman and coworkers demonstrated that selectivity in catalysis can be correlated as a function of the IR spectrum, which makes this analysis timely.[27]

Catalysts **7**–**11**, which form *trans*-cinnamaldehyde-derived iminium ions **2**–**6**, respectively, were employed in the Friedel–Crafts alkylation of *N*-methylpyrrole in a THF/H_2O medium (Table 1). The products were reduced in situ, and the enantiomeric excess (*ee*) values of the products alcohol were determined by HPLC analysis. Reactions proceeding via electron-rich iminium intermediates **2** and **5** (catalysts **7** and **10**) performed best in this transformation, and enantioselectivities of 94 and 90% were obtained, respectively. IRMPD measurements demonstrate that these species adopt stabilizing conformations **I** and **II**, consistent with CH–π and π–π stacking interactions. These interactions have been implicated in the enantiodetermining step of this reaction.[4,6,20] Anthracenyl derivative **9**, proceeding via intermediate **4**, led to lower levels of induction (55%) despite the electron-rich nature of the aryl shielding group that conceivably should allow for stabilizing interactions, as found in **I** and **II**. IRMPD measurements supported by computation indicate that conformation **II** is adopted and that steric repulsion enforces the aromatic moiety to rotate out of plane, which thus erodes shielding. Conformer equivalent **6** (catalyst **11**), in which the phenyl ring is positioned over the π system (i.e., **II**), also populates undesired conformer **IV** and consequently gives lower levels of enantioinduction (63%*ee*). Similarly, catalysis with the use of electron-deficient pentafluorophenyl derivative **8** (iminium salt **3**), which adopts conformation **III**, also gave low levels of enantioselectivity (65%*ee*).

By comparing the IRMPD signatures to catalysis outcomes it is possible to correlate discrete conformers and the molecular space that they occupy to enantioselectivity (Figure 4). The gas-phase structures indicate that population of conformers **I** and **II** facilitates enantioinduction (structures **2** and **5**, 90 and 94%*ee*, respectively). Conversely, population of conformer **III** is detrimental (**3**, 65%*ee*).

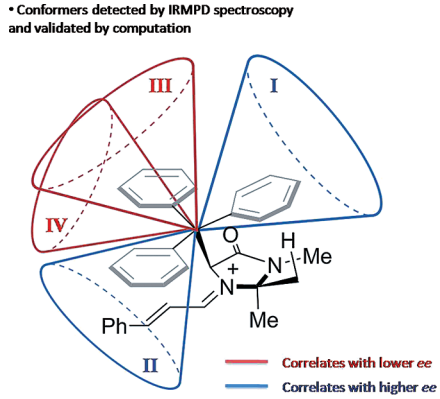

Figure 4. An overview of the IRMPD spectroscopy structure–catalysis correlation.

Table 1. Catalysis screening results with the use of imidazolidinones **7**–**11**.[a]

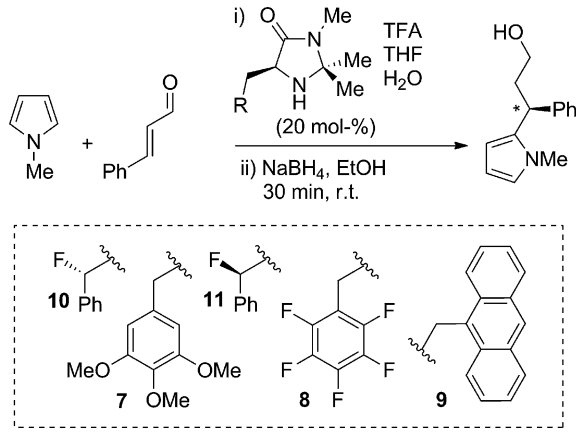

Synthesis		Computation				IRMPD signature	Catalysis *ee*
Catalyst	Salt	Energy of conformers [kJ mol^{-1}]					
		I	**II**	**III**	**IV**		[%]
7	**2**	0.4	0.0	–	0.0	**II**	94
8	**3**	11.8	7.1	0.0		**III**	65
9	**4**	13.2	0.0	18.2	–	**II**	55
10	**5**	0.0	–	–	–	**I**	90
11	**6**	–	0.0		1.3	**II**	63

[a] TFA = trifluoroacetic acid.

Conclusions

In summary, we report a preliminary validation of IRMPD spectroscopic techniques to give structural insights into the complex, charged intermediates that are of central importance to the rapidly developing field of enantioselective organocatalysis. The unique spectroscopic fingerprints gleaned from IRMPD measurements provide new structural data on these well-studied iminium ions in the absence of counterions and solvents (Figure 4). These data, in turn, can be translated into useful guidelines for catalyst design. A preliminary step towards structure–catalysis correlations has been reported in the organocatalytic Friedel–Crafts alkylation of *N*-methylpyrrole.

Supporting Information (see footnote on the first page of this article): Full experimental details and computational details.

Acknowledgments

The authors acknowledge generous financial support from the European Community (FP7/2007-2013; grant number 312284), the Westfälische Wilhelms-Universität Münster, the Deutsche Forschungsgemeinschaft (DFG) (SFB 858), Excellence Cluster EXC 1003 "Cells in Motion – Cluster of Excellence", and the ETH Zürich, Switzerland (ETH Independent Investigator Research Award to R. G.). The authors thank Dr. Britta Redlich and Dr. Lex v. d. Meer for their skilful assistance at the FELIX facility.

[1] a) J. R. Knowles, *Nature* **1991**, *350*, 121–124; b) R. R. Knowles, E. N. Jacobsen, *Proc. Natl. Acad. Sci. USA* **2010**, *107*, 20678–20685.

[2] D. W. C. MacMillan, *Nature* **2008**, *455*, 304–308.

[3] For selected reviews, see: a) M. Nishio, M. Hirota, Y. Umezawa, *The CH/π Interaction: Evidence, Nature and Consequences*, Wiley-VCH, Weinheim, Germany, **1998**; b) J. C. Ma, D. A. Dougherty, *Chem. Rev.* **1997**, *97*, 1303–1324; c) J. P. Gallivan, D. A. Dougherty, *Proc. Natl. Acad. Sci. USA* **1999**, *96*, 9459–9464; d) L. M. Salonen, M. Ellermann, F. Diederich, *Angew. Chem. Int. Ed.* **2011**, *50*, 4808–4842; *Angew. Chem.* **2011**, *123*, 4908–4944.

[4] a) R. Gordillo, J. Carter, K. N. Houk, *Adv. Synth. Catal.* **2004**, *346*, 1175–1185; b) Y. Mori, S. Yamada, *Molecules* **2012**, *17*, 2161–2168.

[5] For selected structural studies on the MacMillan catalyst and iminium derivatives, see: a) C. Burley, R. Gilmour, T. J. Prior, G. M. Day, *Acta Crystallogr., Sect. C* **2008**, *64*, o10–o14; b) D. Seebach, U. Grošelj, M. D. Badine, W. B. Schweizer, A. K. Beck, *Helv. Chim. Acta* **2008**, *91*, 1999–2034; c) U. Grošelj, W. B. Schweizer, M.-O. Ebert, D. Seebach, *Helv. Chim. Acta* **2009**, *92*, 1–13; d) J. B. Brazier, G. Evans, T. J. K. Gibbs, S. J. Coles, M. B. Hursthouse, J. A. Platts, N. C. O. Tomkinson, *Org. Lett.* **2009**, *11*, 133–136; e) D. Seebach, R. Gilmour, U. Grošelj, G. Deniau, C. Sparr, M.-O. Ebert, A. K. Beck, L. B. McCusker, D. Sisak, *Helv. Chim. Acta* **2010**, *93*, 603–634.

[6] M. C. Holland, S. Paul, W. B. Schweizer, K. Bergander, C. Mück-Lichtenfeld, S. Lakhdar, H. Mayr, R. Gilmour, *Angew. Chem. Int. Ed.* **2013**, *52*, 7967–7971; *Angew. Chem.* **2013**, *125*, 8125–8129.

[7] For selected examples of counterion effects influencing reactions outcomes, see: a) M. Lemay, W. W. Ogilvie, *Org. Lett.* **2008**, *10*, 4141–4144; b) D. Marcoux, P. Bindschädler, A. W. H. Speed, A. Chiu, J. E. Pero, G. A. Borg, D. A. Evans, *Org. Lett.* **2011**, *13*, 3758–3761.

[8] a) J. Oomens, B. G. Sartakov, G. Meijer, G. v. Helden, *Int. J. Mass Spectrom.* **2006**, *254*, 1–19; b) N. C. Polfer, J. Oomens, *Mass Spectrom. Rev.* **2009**, *28*, 468–494; c) L. MacAleese, P. Maitre, *Mass Spectrom. Rev.* **2007**, *26*, 583–605.

[9] V. N. Bagratashvili, V. S. Letokov, A. A. Makarov, E. A. Ryabov, *Multiple Photon Infrared Laser Photophysics and Photochemistry*, Harwood, Chichester, UK, **1985**.

[10] W. H. Wing, G. A. Ruff, J. W. E. Lamb, J. Spezeski, *Phys. Rev. Lett.* **1976**, *36*, 1488–1491.

[11] a) M. K. Drayss, D. Blunk, J. Oomens, B. Gao, T. Wyttenbach, M. T. Bowers, M. Schäfer, *J. Phys. Chem. A* **2009**, *113*, 9543–9550; b) K. Asmis, N. L. Pivonka, G. Santambroglio, M. Brümmer, C. Kaposta, D. M. Neumark, L. Wöste, *Science* **2003**, *299*, 1375–1377; c) J. Oomens, B. G. Sartakov, G. Meijer, G. v. Helden, *Int. J. Mass Spectrom.* **2006**, *254*, 1–19; d) N. C. Polfer, J. Oomens, *Mass Spectrom. Rev.* **2009**, *28*, 468–494; e) L. MacAleese, P. Maitre, *Mass Spectrom. Rev.* **2007**, *26*, 583–605.

[12] a) S. H. Yoon, J. Chamot-Rooke, B. R. Perkins, A. E. Hilderbrand, J. C. Poutsma, V. H. Wysocki, *J. Am. Chem. Soc.* **2008**, *130*, 17644–17645; b) J. Oomens, S. Young, S. Molesworth, M. van Stipdonk, *J. Am. Soc. Mass Spectrom.* **2009**, *20*, 334–339.

[13] a) S. A. McLuckey, D. E. Goringer, *J. Mass Spectrom.* **1997**, *32*, 461–474; b) N. Polfer, J. Oomens, *J. Mass Spectrom. Rev.* **2009**, *28*, 468–494.

[14] J. Roithova, *Chem. Soc. Rev.* **2012**, *41*, 547–559.

[15] D. Oepts, A. F. G van der Meer, P. W. van Amersfoort, *Infrared Phys. Technol.* **1995**, *36*, 297–308.

[16] a) M. K. Drayss, D. Blunk, J. Oomens, B. Gao, T. Wyttenbach, M. T. Bowers, M. Schäfer, *J. Phys. Chem. A* **2009**, *113*, 9543–9550; b) A. M. Rijs, I. Compagnon, J. Oomens, J. S. Hannam, D. A. Leigh, W. J. Buma, *J. Am. Chem. Soc.* **2009**, *131*, 2428–2429.

[17] a) A. Ciavardini, F. Rondino, A. Paladini, M. Speranza, S. Fornarini, M. Satta, S. Piccirillo, *Phys. Chem. Chem. Phys.* **2013**, *15*, 19360–19370; b) D. Scuderi, K. Le Barbu-Debus, A. Zehnacker, *Phys. Chem. Chem. Phys.* **2011**, *13*, 17916–17929; c) A. Lagutschenkov, J. Langer, G. Berden, J. Oomens, O. Dopfer, *Phys. Chem. Chem. Phys.* **2011**, *13*, 2815–2823; d) S. Jaeqx, W. Du, E. J. Meijer, J. Oomens, A. M. Rijs, *J. Phys. Chem. A* **2013**, *117*, 1216–1227; e) F. Dreiocker, J. Oomens, A. J. H. M. Meijer, B. T. Pickup, R. F. W. Jackson, M. Schäfer, *J. Org. Chem.* **2010**, *75*, 1203–1213; f) A. R. Massah, F. Dreiocker, R. F. W. Jackson, B. T. Pickup, J. Oomens, A. J. H. M. Meijer, M. Schäfer, *Phys. Chem. Chem. Phys.* **2011**, *13*, 13255–13267.

[18] The components of the traceless quadrupole moment tensor orthogonal to the aromatic ring (Debye-Ångstrom, Q_{zz}) are given for the corresponding toluene derivatives (i.e., Ar-CH_3). Q_{zz} was calculated by using DFT (TPSS/def2-TZVP).

[19] a) C. Sparr, W. B. Schweizer, H. M. Senn, R. Gilmour, *Angew. Chem. Int. Ed.* **2009**, *48*, 3065–3068; *Angew. Chem.* **2009**, *121*, 3111–3114; b) C. Sparr, R. Gilmour, *Angew. Chem. Int. Ed.* **2010**, *49*, 6520–6523; *Angew. Chem.* **2010**, *122*, 6670–6673; c) L. E. Zimmer, C. Sparr, R. Gilmour, *Angew. Chem. Int. Ed.* **2011**, *50*, 11860–11871; *Angew. Chem.* **2011**, *123*, 12062–12074.

[20] A. D. Becke, *J. Chem. Phys.* **1993**, *98*, 5648–5652.

[21] a) A. D. McLean, G. S. Chandler, *J. Chem. Phys.* **1980**, *72*, 5639–5648; b) R. Krishnan, J. S. Binkley, R. Seeger, J. A. Pople, *J. Chem. Phys.* **1980**, *72*, 650–654.

[22] M. J. Frisch, G. W. Trucks, H. B. Schlegel, G. E. Scuseria, M. A. Robb, J. R. Cheeseman, G. Scalmani, V. Barone, B. Mennucci, G. A. Petersson, H. Nakatsuji, M. Caricato, X. Li, H. P. Hratchian, A. F. Izmaylov, J. Bloino, G. Zheng, J. L. Sonnenberg, M. Hada, M. Ehara, K. Toyota, R. Fukuda, J. Hasegawa, M. Ishida, T. Nakajima, Y. Honda, O. Kitao, H. Nakai, T. Vreven, J. A. Montgomery Jr., J. E. Peralta, F. Ogliaro, M. Bearpark, J. J. Heyd, E. Brothers, K. N. Kudin, V. N. Staroverov, R. Kobayashi, J. Normand, K. Raghavachari, A. Rendell, J. C. Burant, S. S. Iyengar, J. Tomasi, M. Cossi, N. Rega, J. M. Millam, M. Klene, J. E. Knox, J. B. Cross, V. Bakken, C. Adamo, J. Jaramillo, R. Gomperts, R. E. Stratmann, O. Yazyev, A. J. Austin, R. Cammi, C. Pomelli, J. W. Ochterski, R. L. Martin, K. Morokuma, V. G. Zakrzewski, G. A. Voth, P. Salvador, J. J. Dannenberg, S. Dapprich, A. D. Daniels, Ö. Farkas, J. B. Foresman, J. V. Ortiz, J. Cioslowski, D. J. Fox, *Gaussian 09*, version D.01, Gaussian, Inc., Wallingford, CT, **2009**.

[23] N. A. Paras, D. W. C. MacMillan, *J. Am. Chem. Soc.* **2001**, *123*, 4370–4371.

[24] For this particular catalysis study, MacMillan and Mayr reported significant counterion effects (see ref.[7]): S. Lakhdar, H. Mayr, *Chem. Commun.* **2011**, *47*, 1866–1868.

[25] D. Seebach, U. Grošelj, W. B. Schweizer, S. Grimme, C. Mück-Lichtenfeld, *Helv. Chim. Acta* **2010**, *93*, 1–16.

[26] For an excellent review on studying noncovalent complexes in the gas phase, see: L. Cera, C. A. Schalley, *Chem. Soc. Rev.* **2014**, *43*, 1800–1812.

[27] A. Milo, E. N. Bess, M. S. Sigman, *Nature* **2014**, *507*, 210–215.

Received: July 1, 2014
Published Online: July 30, 2014

